Journal of Solid Mechanics Vol. 16, No. 2 (2024) pp. 219-245
DOI: 10.60664/jsm.2024.3121796

Research Paper

Thermo-Magneto-Elastic-Plastic Analysis of Functionally Magnetoelastic Pressurized Thick Cylindrical Structure

S. Sohrabi, S. Rash-Ahmadi *

Department of Mechanical Engineering, Urmia University, Urmia, Iran

Received 8 December 2023; Received in revised form 23 August 2024; Accepted 4 September 2024

ABSTRACT

This article explores a semi-analytical method for the Thermo-Magneto-Elastic-Plastic analysis of functionally magnetoelastic (FM) thick cylinders. The FM cylinder is subjected to a uniform magnetic field and combined pressure and temperature loads. Material properties vary radially according to a power-law distribution. The elastic and elastic-plastic distribution of stresses and radial displacement through the radius are obtained. Also, Tresca's yield criterion is used to describe material behavior in plastic zone. The effects of the grading index (β), pressure, temperature, and magnetic intensity vector are discussed. The results indicate that increasing the value of β, internal pressure, external temperature, and magnetic intensity vector lead to the expansion of the yield point from the inner to the outer surface.

Keywords: Functionally graded magnetoelastic cylinder; Thermal analysis; Semi-analytical method; Elastic-plastic; Tresca's criterion.

1 INTRODUCTION

THE increasing need for materials that have high thermal and frictional resistance has led to the development of functionally graded material (FGM). FGMs are composites with non-homogeneous structure that are compared of two or more different materials. Today, studies on FGMs are important because these materials have various applications in industry.

The idea of FGMs was initially suggested by Japanese scientists to convince the requirement of aerospace engineering, for a function of heat shielding, in the mid-1980s [1], [2]. Fukui and Yamanaka [3] investigated the elastic solution of thick-walled cylinders made of functionally graded materials under internal pressure in plane strain and assuming axial symmetry. Jabbari et al [4] presented an analytical solution for the calculation of the axisymmetric thermal and mechanical stresses in a thick-walled hollow cylinder made of FGM. The authors have

*Corresponding author. Tel.: +98 44 31942855.
E-mail address: s.rashahmadi@urmia.ac.ir (Samrand Rash-Ahmadi)

obtained the thermal and mechanical stresses through the direct method of solving the Navier equation. Tutuncu and Ozturk [5] studied the elastic behavior of FG cylinder and sphere under internal pressure using infinitesimal elasticity theory. They assumed that the hardness of the material changes exponentially with thickness. In this study, Poisson's ratio is assumed as constant and the stress distribution is compared with the homogeneous state depending on the strength index. Eslami et al [6] considered a thick hollow sphere of FGM under one-dimensional steady-state temperature distribution with general types of boundary conditions (thermal and mechanical). Abrinia et al [7] examined the thermoelastic behavior of a thick-walled cylinder made of FG material under internal temperature and pressure by assuming a power function for the modulus of elasticity and coefficient of thermal expansion. Peng and Li [8] analyzed the elastic behavior of an axisymmetric FGM hollow disk or cylinder. Peng and Li [9] investigated the thermoelastic analysis for axisymmetrical problems of an FGM hollow cylinder. Li et al [10] presented analytical solutions for deformation and stress distribution in FGM beams with variable thicknesses. Nie et al [11] considered the tailoring of volume fractions of constituents in FG hollow cylinders and spheres to realize either through the thickness uniform hoop stress or in plane shear stress Seifi [12] analyzed the thermoelastic behavior of the thick-walled FG cylinder in two states of power and exponential functions for changes in material properties. They used two methods, namely the analytical exact and the approximate homogenous multilayer semi-analytical methods. Their results were shown that approximate semi-analytical homogenous multilayer is simple and has appropriate results. Chen [13] investigated the stress changes in a rotating, spherically isotropic, FGM spherical shell. In this article, the material properties were defined as a function of radius. Allam et al [14] the semi-analytical solution for stress distribution in inhomogeneous and FG rotating disks with variable thickness. They considered two specific thickness variation namely power and exponent laws for thickness variation. The main conclusion of this paper was that the semi-analytical solution is an accurate and reliable. Xie et al [15] studied a uniform form of the basic equations of the FG hollow cylinder/spherical shell by introducing parameter δ and further discussed the stress distribution of the FG cylindrical/spherical shell under three different boundary conditions. Abdalla et al [16] analyzed the thermo-mechanical stresses in FG axisymmetric rotating hollow disks when the thickness is not constant.

Magnetoelastic materials are widely used in various application such as lasers, microwave and ultrasonic devices. Using the infinitesimal magnetoelastic theory, Dai, Fu and Dong [17] analyzed the magnetoelastic behavior of a FG cylindrical and spherical vessels located in a magnetic field and under internal pressure. Then they have shown that the inhomogeneity parameter has a significant effect on the stress and disturbance of the magnetic field. Also, in another article, Dai and Fu [18] investigated the magneto thermoelastic behavior of a FG cylinder and a hollow sphere placed in a magnetic, thermal field and under mechanical loading. Using the infinitesimal magnetoelastic theory, Ghorbanpour et al [19] derived the governing equation of the FG rotating hollow disk and presented a semi-analytical solution for temperature, radial and hoop stresses and radial displacement. They compared the results with and without a magnetic field under different boundary conditions and have shown that by applying the magnetic field, the environmental stress is significantly reduced and, as a result, fatigue life is improved. The effect of the magnetic field on the thermoelastic behavior of the rotating disk with non-uniform thickness between two states of stable and unstable temperature field was investigated by Sarkar et al [20]. By using higher-order shear deformation theory, Nejad et al [21] conducted a thermo-elastic analysis of a functionally graded rotary thick shell with arbitrary curvature and variable thickness under thermomechanical loading.

Eraslan and Akis [22] extracted the governing equations of the FG cylinder under elastic and elastic-plastic pressure under the condition of plane strain by using Tresca's criterion and the theory of small deformations. They assumed the modulus of elasticity and yield limit vary radially according to general parabolic forms and used the Tresca's yield criterion. Akis [23] investigated purely elastic, partially plastic and fully plastic stress states of internally pressurized FG spherical pressure vessels. By using Tresca's yield criterion, Ozturk et al [24] examined elastic-plastic deformation of a solid cylinder with uniform internal heat generation and the end is fixed. They indicated that material non-homogeneity has an essential effect on the stress distributions in solids. However, the result obtained show that the stress distribution, as well as the development of plastic region radii, is influence substantially by the material non-homogeneity. Rash Ahmadi et al [25] presented a numerical solution to investigate the elastic-plastic behavior of the spherical pressure vessel by assuming the non-linear change of the modulus of elasticity in the direction of the radius. The authors used a semi-analytical method to solve the governing equations. Nejad et al [26] investigated the elastic-plastic deformation and stresses in the FG rotating disk. They assumed the material properties to vary according to the power-law and presented the stresses and deformations of three different plastic regions using Tresca's yield condition. Alikarami and Parvizi [27] presented an exact closed-form analytical elasto-plastic solution for thick-walled FG cylinder subjected to combined pressure and temperature gradient loadings. In the study based on the experimental results, a mathematical model was developed to predict the yield.

They found that under the temperature gradient, there are points in the cylinder where the environmental stress changes from compressive to tensile. The position of this point is independent of the temperature gradient and depends on the geometry and material properties of the cylinder. Pengpeng Shi and Jun Xie[28] presented an exact elastoplastic solution for an FG cylinder subjected to internal pressure. They assumed the modulus of elasticity changes as a power function and Poisson's ratio is assumed as constant. They found that plastic deformation may appear from the inner radius or outer radius.

In this work, the functionally magnetoelastic thick cylinder with constant thickness placed in a uniform magnetic field and under combined pressure and temperature loads is presented. the material's thermal, mechanical and magnetic properties excepted Poisson's ratio varies radially according to power-law distribution. A semi-analytical method is applied to obtain the Thermo-Magneto-Elastic and Thermo-Magneto-Elastic-Plastic solutions of FM cylinder. In the section of Thermo-Magneto-Elastic-Plastic, Tresca's yield criterion is used to describe material behavior in plastic zone. The effect of grading index, temperature and pressure on stresses and radial displacement were also investigated.

2. GRADATION RELATION

The material properties, expect Poisson's ratio vary continuously and smoothly in the direction r. despite this, the most commonly model is power-law distribution of the volume fraction. In this study, a material property $'q(r)'$ is given by

$$q(r) = (q_o - q_i)\left(\frac{r - r_i}{r_o - r_i}\right)^{\beta} + q_i \qquad r_i < r < r_o \tag{1}$$

Where q_o and q_i disclose the property of the outer and inner radius of the FM cylinder, respectively. Not that, the parameter β is a grading index (or inhomogeneity parameter) which takes positive value. Using Equation (1) the variation of the elasticity modulus $E(r)$, thermal coefficient of expansion $\alpha(r)$, heat conductivity $K(r)$, magnetic permeability $\mu(r)$ and yield stress $\sigma_y(r)$ in the rang $r_i < r < r_o$ are obtained.

3. THERMO-ELASTIC EQUATIONS

It is assumed that the Poisson's ratio (υ) takes a constant value and cylindrical coordinate system (r, θ, z) is used. The present study focuses on the Magnetic-Thermo-Elastic-Plastic analysis of a FM cylinder with a constant and thick thickness, inner radius r_i, outer radius r_o and plane strain condition. The magnetic cylinder placed in a uniform magnetic field with magnetic intensity vector $\bar{H}(0,0, H_z)$ and under mechanical and thermal loading. The considered FM cylinder is made of a metal and a ceramic at the inside and outside surfaces, respectively.

The one-dimensional and steady-state temperature distribution model in cylindrical system without heat generation reads

$$\frac{1}{r}\frac{d}{dr}\left(rK(r)\frac{dT_r}{dr}\right) = 0, \qquad r_i < r < r_o \tag{2}$$

Equation (2) can be expanded as

$$A_1\frac{d^2T_r}{dr^2} + A_2\frac{dT_r}{dr} = 0 \tag{3}$$

where

$$A_1 = rK(r) \tag{4}$$

$$A_2 = K(r) + r\frac{dK}{dr}$$

T_r and $K(r)$ are the radial temperature and thermal conduction coefficient. $K(r)$ is defined according to Equation

$$K(r) = (K_o - K_i)\left(\frac{r - r_i}{r_o - r_i}\right)^{\beta} + K_i \qquad r_i < r < r_o \tag{5}$$

(1).

Due to complication of coefficient, a semi-analytical method is used. For this purpose, the cylinder is divided into some finite sub-domains with constant thickness t, as shown in Figure 1. The coefficients of Equation (3) are assessed at $r^{(j)}$, mean radius of *jth* division and the ODE problem with constant coefficient in *jth* sub-domain is rewritten as bellow:

$$\left(A_1^{(j)}\frac{d^2}{dr^2} + A_2^{(j)}\frac{d}{dr}\right)T_r^{(j)} = 0 \tag{6}$$

Now we have got *N* ODEs with constant coefficients. Therefore, the exact answer for Equation (5) can be written in the form of:

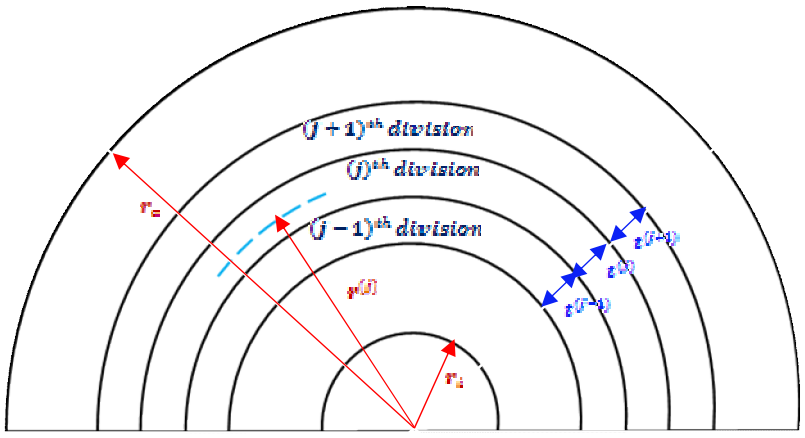

Fig. 1
Dividing radial domain into some finite sub-domains.

$$T_r^{(j)} = X_1^{(j)} + X_2^{(j)} \exp\left(-r\frac{A_2^{(j)}}{A_1^{(j)}}\right) \tag{7}$$

Where $X_1^{(j)}$ and $X_2^{(j)}$ are unknown constant for sub domain *(j)* which are determined by applying the boundary conditions between two adjacent layers. For the sake, the continuity and global thermal conditions are

$$T_r|_{r=r^{(j)}+\frac{t}{2}} = T_r|_{r=r^{(j+1)}-\frac{t}{2}} \tag{8}$$

$$\left.\frac{dT_r}{dr}\right|_{r=r^{(j)}+\frac{t}{2}} = \left.\frac{dT_r}{dr}\right|_{r=r^{(j+1)}-\frac{t}{2}}$$

$$T_r|_{r=r_i} = T_i, \qquad T_r|_{r=r_o} = T_o$$

These conditions give a set of linear algebraic equation in terms of $X_1^{(j)}$ and $X_2^{(j)}$. Solving the resultant equation for $X_1^{(j)}$ and $X_2^{(j)}$, the unknown coefficients of Equation (7) are calculated. Then T_r is determined in each sub-domain.

4. MAGNETO-THERMO-ELASTIC ANALYSIS OF FM CYLINDER

The cylinder towards the z-axisymmetric. We have got the radial displacement which is independent of θ and *z*. So, the constitutive relations are

$$\varepsilon_r = \frac{du_r}{dr}, \varepsilon_\theta = \frac{u_r}{r}, \varepsilon_z = 0 \tag{9}$$

$$\sigma_r = \frac{E(r)}{(1-\upsilon^2)}\left(\varepsilon_r + \upsilon\varepsilon_\theta - \alpha(r)T_r(1+\upsilon)\right) \tag{10}$$

$$\sigma_\theta = \frac{E(r)}{(1-\upsilon^2)}\left(\upsilon\varepsilon_r + \varepsilon_\theta - \alpha(r)T_r(1+\upsilon)\right) \tag{11}$$

$$\sigma_z = \upsilon(\sigma_r + \sigma_\theta) \tag{12}$$

The Equilibrium equation in the present of magnetic body force has the form

$$\frac{d\sigma_r}{dr} + \frac{\sigma_r - \sigma_\theta}{r} + f_z = 0 \tag{13}$$

Where [29]

$$f_z = \mu(r){H_z}^2\frac{d}{dr}\left(\frac{du_r}{dr} + \frac{u_r}{r}\right) \tag{14}$$

Is defined as Lorentz's force and the variation of properties are determined in section (1). Substituting material properties, stresses from Equations (10-11) and Lorentz's force from Equation (14) into equilibrium Equation (13), Magneto-Thermo-Elastic equation are obtained as follow:

$$C_1\frac{d^2u_r}{dr^2} + C_2\frac{du_r}{dr} + C_3u_r + C_4 = 0 \tag{15}$$

Where

$$C_1 = r\left(E(r) + \left(\mu(r)H_z^2(1-\nu^2)\right)\right) \tag{16}$$

$$C_2 = r\frac{dE(r)}{dr} + E(r) + \left(\mu(r)H_z^2(1-\nu^2)\right)$$

$$C_3 = \nu\frac{dE(r)}{dr} - \frac{1}{r}\left(E(r) + \mu(r)H_z^2(1-\nu^2)\right)$$

$$C_4 = -r(1+\nu)\left(\frac{dE(r)}{dr}\alpha(r)T_r + E(r)\frac{d\alpha(r)}{dr}T_r + E(r)\alpha(r)\frac{dT_r}{dr}\right)$$

For the solve differential Equation (15), again, the semi-analytical method is used as previously explained. The Equation (15) can be rewritten as

$$\left(C_1^{(j)}\frac{d^2}{dr^2} + C_2^{(j)}\frac{d}{dr} + C_3^{(j)}\right)u_r^{(j)} + C_4^{(j)} = 0 \tag{17}$$

The solution is

$$u_r^{(j)} = X_3^{(j)}\exp\left(\kappa_1^{(j)}r\right) + X_4^{(j)}\exp\left(\kappa_2^{(j)}r\right) - \frac{C_4^{(j)}}{C_3^{(j)}} \tag{18}$$

Where

$$\kappa_1^{(j)}, \kappa_2^{(j)} = -\frac{C_2^{(j)} \pm \sqrt{\left(C_2^{(j)}\right)^2 - 4C_3^{(j)}C_1^{(j)}}}{2C_1^{(j)}} \tag{19}$$

The unknown constant $X_3^{(j)}$ and $X_4^{(j)}$ are the integral coefficients for *jth* division. In order to find these constant, boundary conditions are

$$u_r^{(j)}\Big|_{r=r^{(j)}+\frac{t}{2}} = u_r^{(j+1)}\Big|_{r=r^{(j+1)}-\frac{t}{2}} \tag{20}$$

$$\sigma_r^{(j)}\Big|_{r=r^{(j)}+\frac{t}{2}} = \sigma_r^{(j+1)}\Big|_{r=r^{(j+1)}-\frac{t}{2}}$$

$$\sigma_r|_{r=r_i} = -P_{in},\ \sigma_r|_{r=r_o} = -P_{out}$$

$X_3^{(j)}$ and $X_4^{(j)}$ of Equation (20) are calculated by applying the continuity and boundary conditions simultaneously. Then u_r is determined in each sub-domain. By substituting $u_r^{(j)}$ into Equation's (10-12), the stresses in each layer are calculated.

5. INITIAL YIELDING

In the present analysis, Tresca's criterion is used to determine the yield condition. Since $\sigma_\theta \geq \sigma_z \geq \sigma_r$ throughout the cylinder, Tresca's yield form of

$$\sigma_\theta - \sigma_r = \sigma_y \tag{21}$$

Rewriting Equation (21) into non-dimensional form gives

$$\phi_Y = \frac{\sigma_\theta - \sigma_r}{\sigma_y} \tag{22}$$

Substituting Equation's (10-11) into Equation (21), the starting point of yield is obtained. Not that there are three different situations for boundary conditions. By changing parameters, the yield may start from the inside, outside or simultaneously from inside and outside (shown in Figure 2).

$$\phi_Y \begin{cases} < 1 \rightarrow & elastic\ region \\ = 1 \rightarrow & when\ yeild\ happen \\ > 1 \rightarrow & plastic\ flow\ begins \end{cases}$$

First, the general equation of solution is presented. Then, the problem is solved separately for the different mode of plastic flow (all three cases).

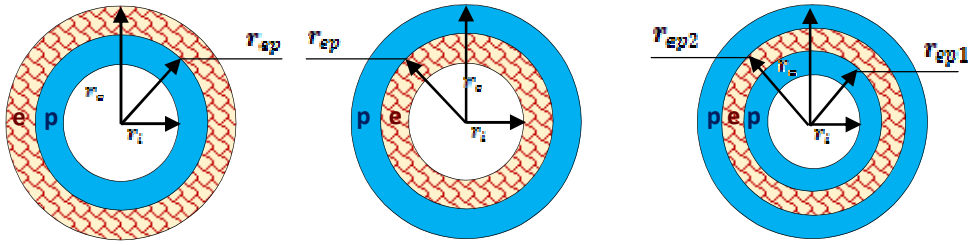

Fig. 2
Plastic region initiates from (a) the inner radius, (b) the outer radius, and (c) both.

6. MAGNETO-THERMO-ELASTIC-PLASTIC ANALYSIS OF FM CYLINDER

Again, semi-analytical method has been used for this section. The plastic stresses by substituting Equation (21) into Equation (13) are determined to be

$$\left(\sigma_r^p\right)^{(j)} = \sigma_y^{(j)} Lnr - f_z^{(j)} r + X_5{}^{(j)} \tag{23}$$
$$\left(\sigma_\theta^p\right)^{(j)} = \sigma_y^{(j)} (Lnr + 1) - f_z^{(j)} r + X_5{}^{(j)}$$
$$\left(\sigma_z^p\right)^{(j)} = v\left(\sigma_r^p + \sigma_\theta^p\right)^{(j)}$$

Where

$$f_z^{(j)} = \mu(r) H_z{}^2 \left(\frac{d^2}{dr^2} + \frac{1}{(r^{(j)})^2}\left(r^{(j)} \frac{d}{dr} - 1\right)\right) u_r^{(j)} \tag{24}$$
$$\sigma_y^{(j)} = (\sigma_{yo} - \sigma_{yi}) \left(\frac{r^{(j)} - r_i}{r_o - r_i}\right)^\beta + \sigma_{yi}$$

And X_5 is an integration constant. Notice that, superscript p denote plastic. Solving this elastic-plastic problem requires the evaluation of four unknown constants: X_3, X_4, r_{ep} and X_5.

6.1 Case1: yielding initiation from the inside

If the yield starts from the inner surface. The plastic region is cylindrical with inner radius r_i and outer radius r_{ep}. The boundary and continuity conditions for calculation of integration constant (X_5) are

$$\sigma_r^p\big|_{r=r_i} = -P_{in} \tag{25}$$
$$(\sigma_r^p)^{(j)}\Big|_{r=r^{(j)}+\frac{t}{2}} = (\sigma_r^p)^{(j+1)}\Big|_{r=r^{(j+1)}-\frac{t}{2}}$$

By applying the boundary condition X_5 is calculated in the first layer. Then, integration constant in each layer can be obtained using the value of X_5 in the previous layer.

$$X_5^{(j+1)} = Lnr\left(\sigma_y^{(j)} - \sigma_y^{(j+1)}\right) + r\left(f_z^{(j+1)} - f_z^{(j)}\right) + X_5^{(j)} \qquad j=1, 2, ..., N \tag{26}$$

Substituting Equation (26) into Equation (23), the plastic stresses in each layer are calculated. The constants of elastic part are determined by using continuity conditions of stress in the boundary of elastic-plastic region.

$$\sigma_r^e\big|_{r=r_{ep}} = \sigma_r^p\big|_{r=r_{ep}} \tag{27}$$
$$\sigma_r^e\big|_{r=r_o} = -P_o$$

Making use of these expressions, the stress-strain relations and the associated flow rule $\varepsilon_r^p + \varepsilon_\theta^p = 0$, the sum of total radial and hoop strains, we arrive that

$$\frac{du_r}{dr} + \frac{u_r}{r} = \frac{1-\nu}{E(r)}(2\sigma_r + \sigma_y) + 2\alpha(r)T_r \tag{28}$$

By applying semi-analytical method, The Equation (28) can be rewritten as

$$\left(\frac{d}{dr} + D_1^{(j)}\right)u_r^{(j)} = D_2^{(j)} \tag{29}$$

Where

$$D_1^{(j)} = \frac{1}{r} \tag{30}$$
$$D_2^{(j)} = \frac{1-\nu}{E^{(j)}}\left(2\sigma_r^{(j)} + \sigma_y^{(j)}\right) + 2\alpha^{(j)}T_r^{(j)}$$

The solution is

$$u_r^{(j)} = \frac{D_1^{(j)}}{D_2^{(j)}} - \frac{X_6^{(j)}}{exp\left(rD_1^{(j)}\right)} \tag{31}$$

The continuity conditions between two adjacent layers in the plastic region and the continuity between the plastic and elastic regions for calculation of integration constant (X_6) is

$$(u_r^p)^{(j)}\Big|_{r=r^{(j)}+\frac{t}{2}} = (u_r^p)^{(j+1)}\Big|_{r=r^{(j+1)}-\frac{t}{2}} \tag{32}$$
$$u_r^e\big|_{r=r_{ep}} = u_r^p\big|_{r=r_{ep}}$$

6.2 Case2: yielding initiation from the outside

If the yield starts from outer surface. Elastic region in $r_i < r < r_{ep}$ and the plastic region in $r_{ep} < r < r_o$. The boundary and continuity conditions to obtain X_3 as follows

$$\sigma_r^p\big|_{r=r_o} = -P_o \tag{33}$$
$$\left(\sigma_r^p\right)^{(j)}\Big|_{r=r^{(j)}+\frac{t}{2}} = \left(\sigma_r^p\right)^{(j+1)}\Big|_{r=r^{(j+1)}-\frac{t}{2}}$$

$$X_3^{(j)} = Lnr\left(\sigma_y^{(j-1)} - \sigma_y^{(j)}\right) + r\left(f_z^{(j)} - f_z^{(j-1)}\right) + X_3^{(j-1)} \qquad j=N, N-1, \ldots, 1 \tag{34}$$

Substitution will result

By applying the boundary condition X_3 is calculated in the end layer. Then, integration constant in each layer can be obtained using the value of X_3 in the previous layer.

6.3 Case3: yielding initiation from the inside and outside, simultaneously

In case the yield starts simultaneously from the inner and outer surface. The elastic region is cylindrical with inner radius r_{ep1} and outer radius r_{ep2}. Elastic and plastic constants are calculated from boundary and continuity conditions as follows

$$\sigma_r^p\big|_{r=r_i} = -P_{in} \tag{35}$$
$$\left(\sigma_r^p\right)^{(j)}\Big|_{r=r^{(j)}+\frac{t}{2}} = \left(\sigma_r^p\right)^{(j+1)}\Big|_{r=r^{(j+1)}-\frac{t}{2}}$$
$$\sigma_r^e\big|_{r=r_{ep1}} = \sigma_r^p\big|_{r=r_{ep1}}$$
$$\sigma_r^e\big|_{r=r_{ep2}} = \sigma_r^p\big|_{r=r_{ep2}}$$

7. RESULTS AND DISCUSSION

In this study, the following non-dimensional variables are used to present numerical results:

$$\bar{r} = \frac{r}{r_o}\ ; \quad \bar{\sigma}_j = \frac{\sigma_j}{\sigma_y(r=r_i)}\ ; \quad \bar{u}_j = \frac{u_j E(r=r_i)}{r_o \sigma_y(r=r_i)};$$

7.1 Verification

In order to verification method, the numerical results are compared with Erasalan and Akis for a FGM tube under internal pressure. In this reference (18) variation of modulus of elasticity and the yield limit was described as follows:

$$E = E_0\left[1 - n\left(\frac{r}{b}\right)^k\right] \tag{36}$$

$$\sigma_Y = \sigma_0\left[1 - m\left(\frac{r}{b}\right)^s\right]$$

The comparison between non-dimensional stresses in the radial direction using semi-analytical method and the results based on reference (18) for

$\frac{a}{b} = 0.7, n = 0.348459,\ k = -0.7, m = 0.7\ and\ s = 1.1$

under internal pressure $\bar{P}_{in} = 0.28$ is shown in Figure 3. It is noted that the results have good accuracy with literature.

In this section, the influence of grading index, pressure, temperature and magnetic intensity vector on stresses and radial displacement are studied. The material properties of Aluminum as inner surface and Zirconia as outer surface are summarized in Table 1 [30], [31]. The Poisson's ratio $\nu = 0.3$ and radius ratio $\frac{r_i}{r_o} = 0.7$ are also taken to be the same of reference (18). Not that, temperature gradient in the FM cylinder is subjected positive $(T_o > T_i)$.

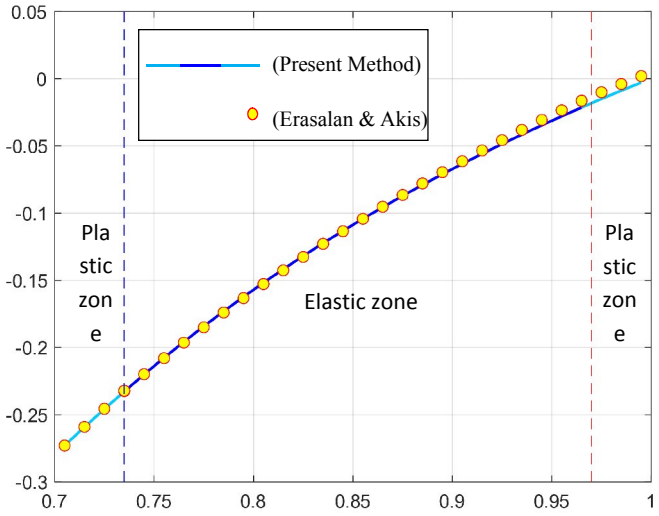

Fig. 3
Vilification present method with reference.

Table 1.
Properties of Functionally magnetoelastic cylinder.

Geometry property	Inner surface		0.7
	Outer surface		1
Mechanical properties	Young's modulus (Gpa)	Inner surface	70
		Outer surface	115
	Yield stress (Mpa)	Inner surface	278
	Ultimate strength (Mpa)	Outer surface	1030
thermal properties	Thermal expansion coefficient $(1/℃)$	Inner surface	23×10^{-6}
		Outer surface	8×10^{-6}
	Thermal conductivity $(W/m°K)$	Inner surface	237
		Outer surface	22.7
Magnetic properties	Magnetic probability (H/m)	Inner surface	$1.256665081 \times 10^{-6}$
		Outer surface	$1.256665081 \times 10^{-6}$
	Magnetic intensity (A/m)		2.23×10^{9}

7.2 Magneto-Thermo-Elastic results

The radial, hoop stresses and radial displacement in the elastic FM cylinder subjected to $P_i = 5Mpa, P_o = 0, T_i = 0$ and $T_o = 5\,℃$ for three values of grading index are presented in Figures 4–6. From these figures, the maximum and minimum stresses and radial displacement are located near the inner and outer surface of the FM cylinder, respectively. It is observed from Figures 4 and 5 that the grading index significantly influences the stresses. Figure 4 shows that an increasing in β , yields compressive radial stresses in the cylinder.

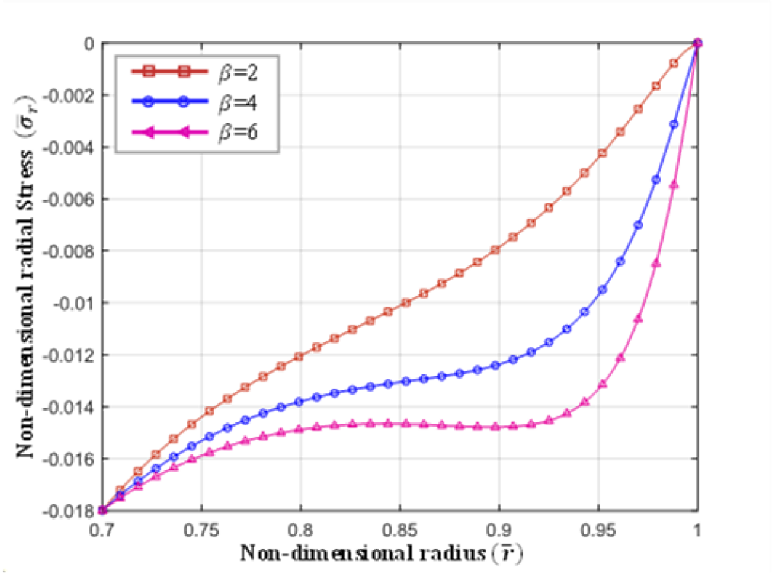

Fig. 4
Radial stress in Magneto-Thermo-Elastic FM cylinder.

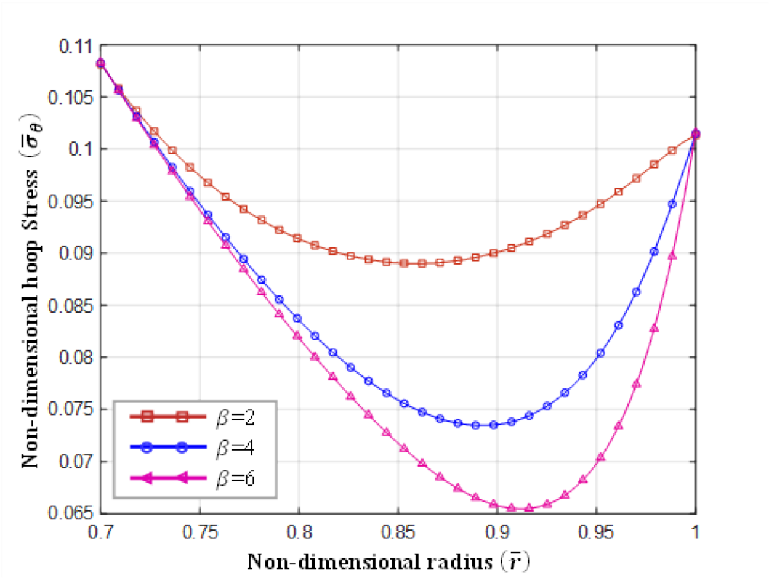

Fig. 5

Hoop stress in Magneto-Thermo-Elastic FM cylinder.

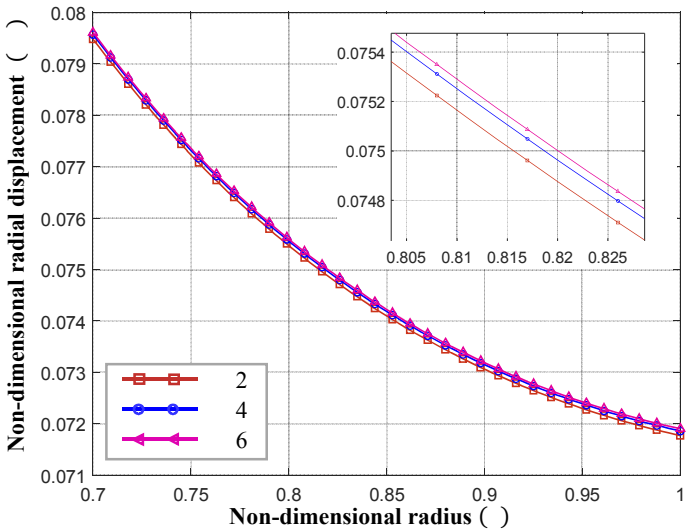

Fig. 6
Radial displacement in Magneto-Thermo-Elastic FM cylinder.

7.3 Magneto-Thermo-Elastic-Plastic results

In this section, the Elasto-plastic analysis of FM cylinder is presented. The results occur due to $P_i = 120Mpa, P_o = 0, T_i = 0$ and $T_o = 50\ ^\circ C$. In order to find the yield initiation point, the changes of dimensionless parameter Φ in the radial direction for different values of β are shown in Figure 7.

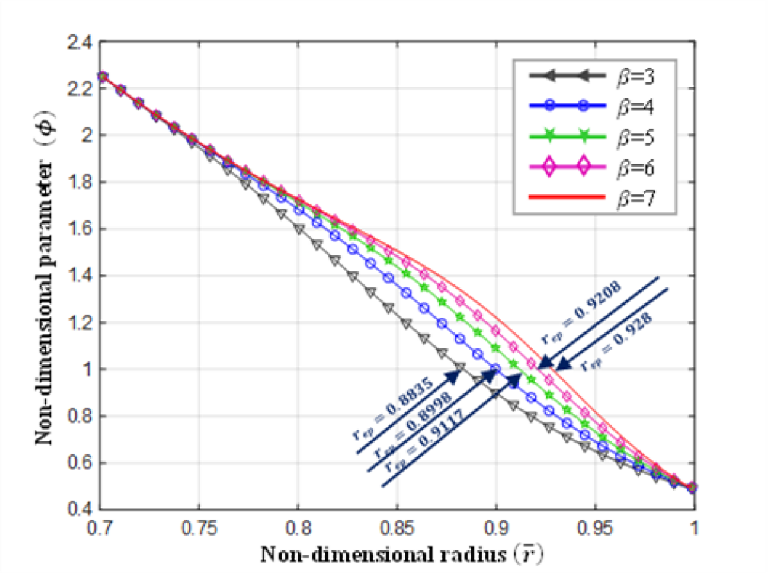

Fig. 7
Changes of dimensionless parameter ϕ for different value of β.

It is seen that, increasing the value of β expands the yield point from inner to outer surface. stresses along the radius direction for different value of grading index β are provided in Figures 8–10. Not that, the dashed-lines are used to indicate the plastic region and solid-lines are used to the elastic region.

One known from the curves of Figure 8 that by increasing β the plastic zone is increased and the amount of radial stress is decreased. This Figure illustrates that an increasing β yields compressive radial stresses in the cylinder. It is seen from the curves of Figure 9 that the value of hoop stress decrease as the increasing of β. Figure 10 illustrate the distribution of axial stress and its similar that of Figure 9.

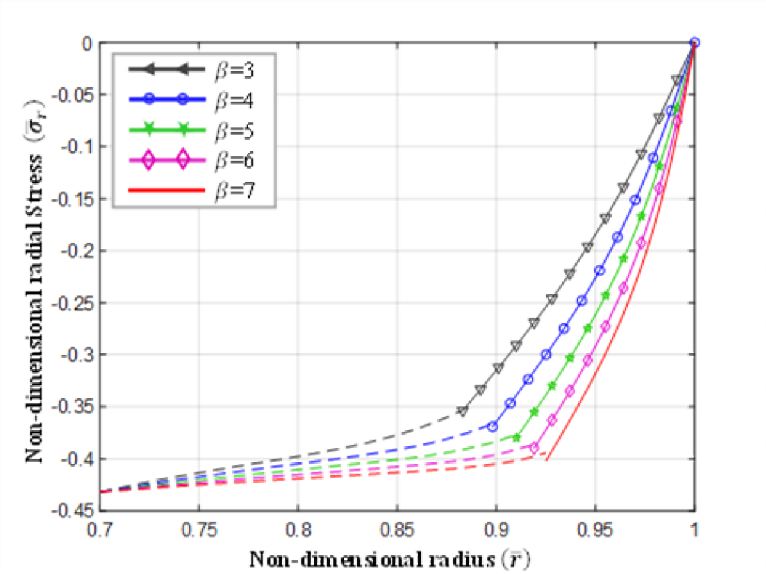

Fig. 8
Radial stress in Magneto-Thermo-Elastic-Plastic FM cylinder.

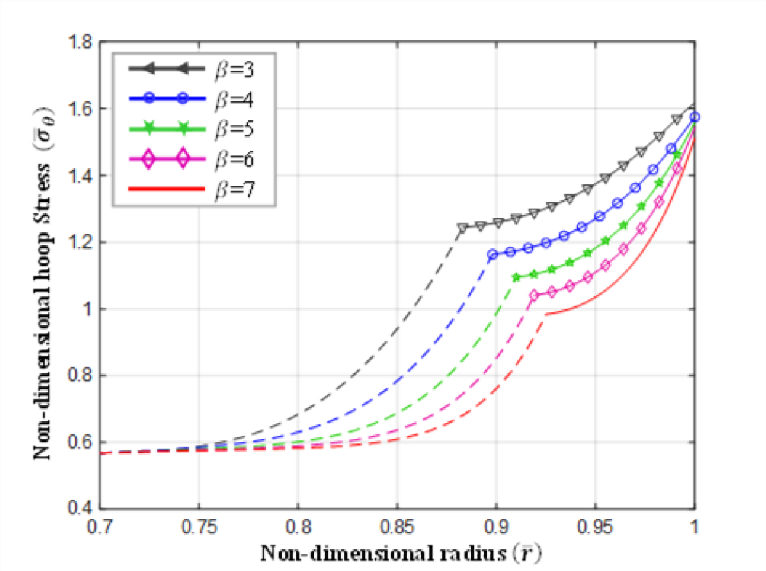

Fig. 9
Hoop stress in Magneto-Thermo-Elastic-Plastic FM cylinder.

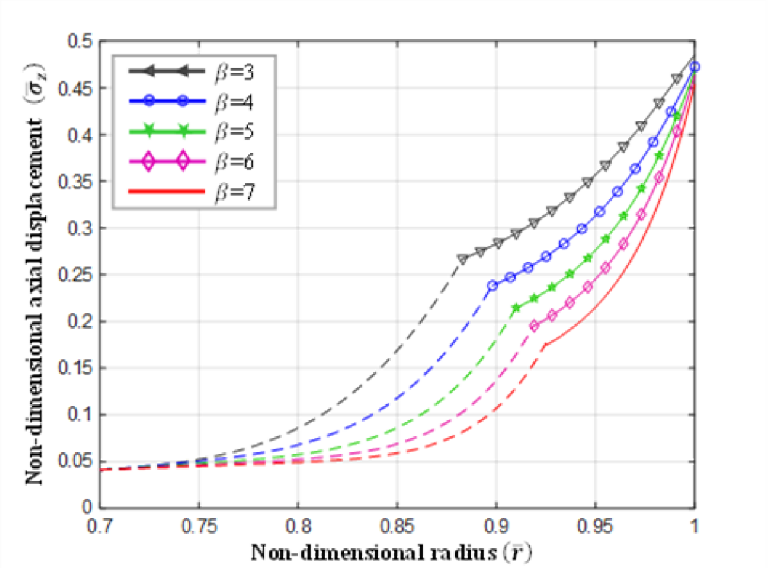

Fig. 10
Axial stress in Magneto-Thermo-Elastic-Plastic FM cylinder.

Figure11 depicts the non-dimensional radial displacement. This figure show that the value of the radial displacement decreases as the increasing of β.

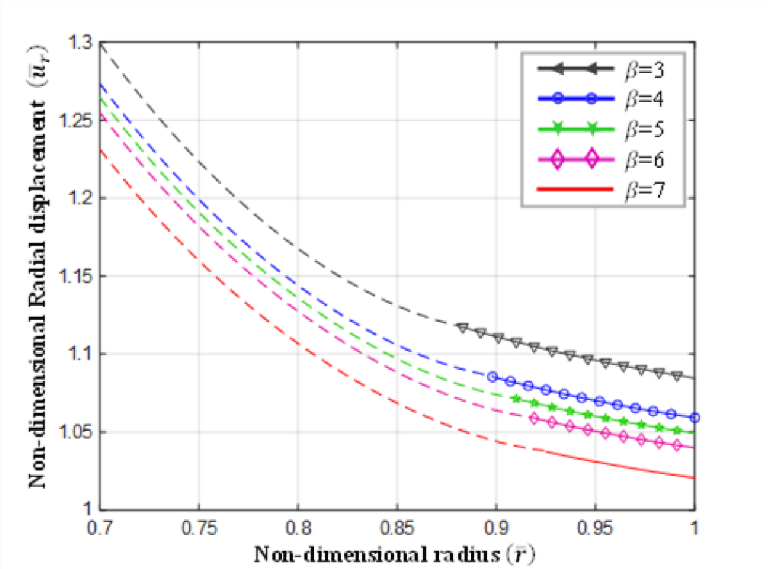

Fig. 11
Radial displacement in Magneto-Thermo-Elastic-Plastic FM cylinder.

Figures 12–15 show the effect of various external temperature on dimensionless parameter ϕ, radial and hoop stresses and radial displacement where $P_i = 120Mpa, P_o = 0, T_i = 0, T_o = 30,50,70,90$ and $110°C$. According to Figure 12, the variation of the dimensionless parameter ϕ near the outer surface becomes small for high external temperature. One known from the curves of Figure 13 that by decreasing T_o, the absolute values of the radial stress decreases and it becomes more uniform along the radius. In functionally graded materials, different layers may have varying coefficients of thermal expansion. The FM cylinder consists of aluminum on the inner surface and zirconia on the outer surface. Zirconia has a lower expansion coefficient compared to aluminum. When the FM cylinder is exposed to an external temperature, the difference in expansion coefficients between the layers can result in hoop and radial stresses. It can be observed from the curves in Figure 13 that changes in expansion ultimately lead to a reduction in the absolute value of radial stress from the inner surface to the outer surface. Figure 14 shows that by increasing T_o, the hoop stress decreases in the plastic region and increases in the elastic region. Not that, the grading index is equal to 3 $(\beta = 3)$ in Figures 12–27.

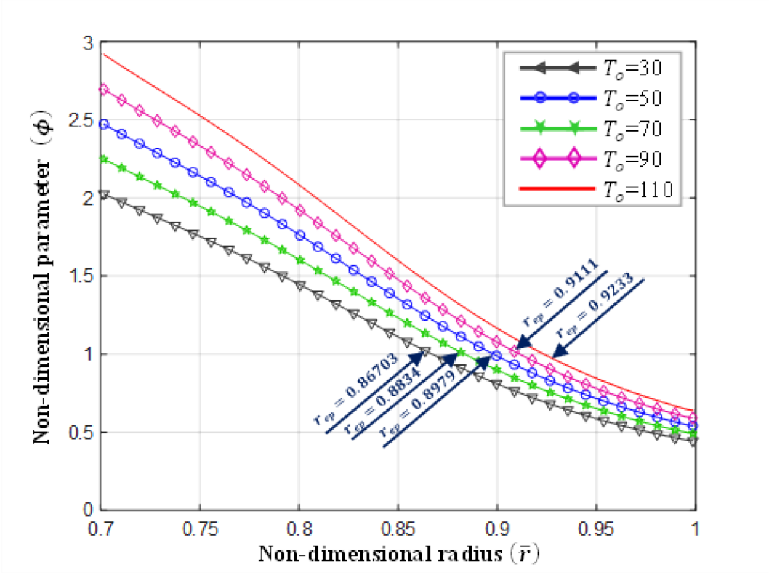

Fig. 12
Changes of dimensionless parameter ϕ for different external temperature.

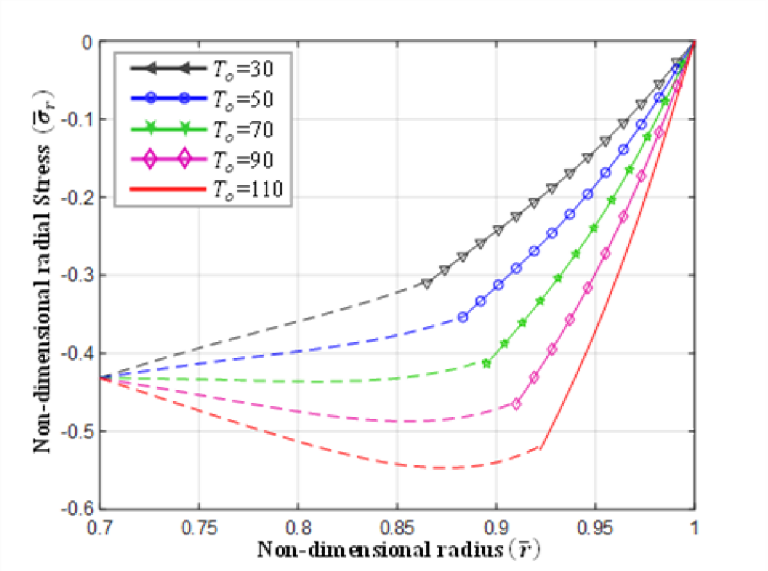

Fig. 13
Radial stress in Magneto-Thermo-Elastic-Plastic FM cylinder for different external temperature.

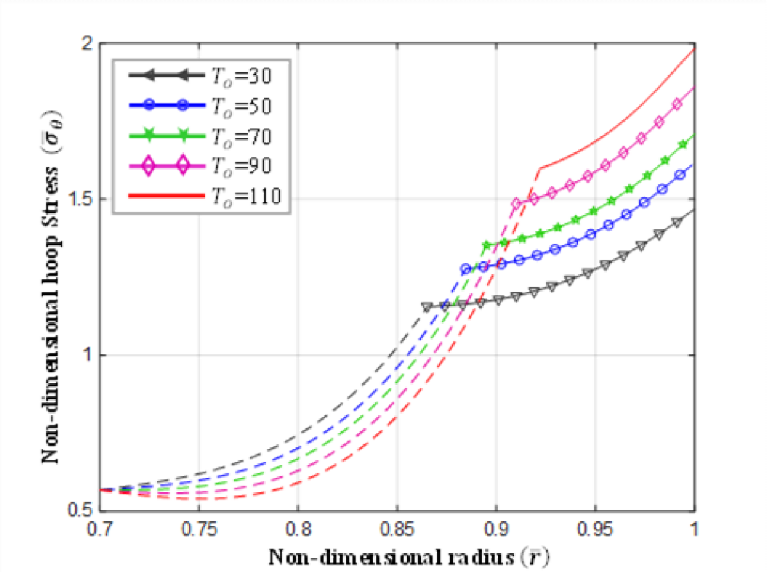

Fig. 14
Hoop stress in Magneto-Thermo-Elastic-Plastic FM cylinder for different external temperature.

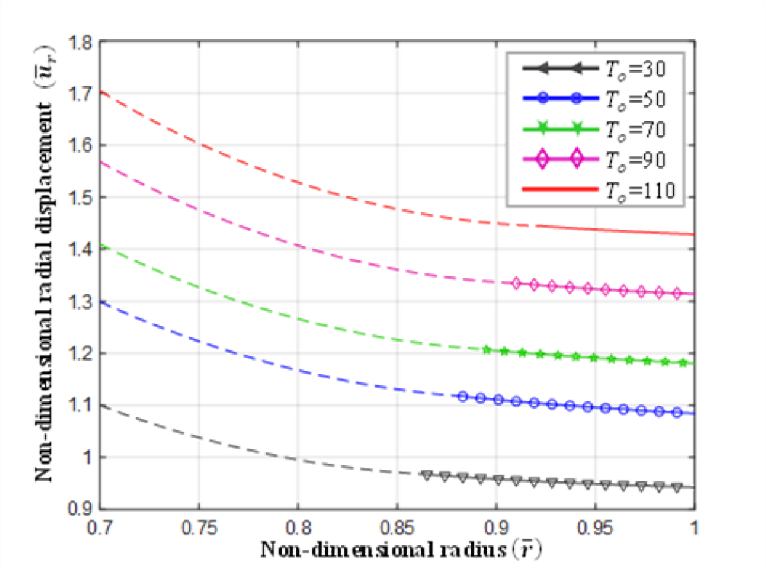

Fig. 15
Radial displacement in Magneto-Thermo-Elastic-Plastic FM cylinder for different external temperature.

The effect of internal pressure on dimensionless parameter ϕ, radial and hoop stresses and radial displacement are introduced in Figures 16–19. The results occur due to $T_i = 0, T_o = 50°C, P_o = 0, P_i = 100, 110, 120, 130$ and 140Mpa. According to Figure 16, The variation of the dimensionless parameter ϕ follows a trend similar to the change in the dimensionless parameter with external temperature. Figure 18 shows that by increasing P_i, the hoop stress decreases in the plastic region and increases in the elastic region.

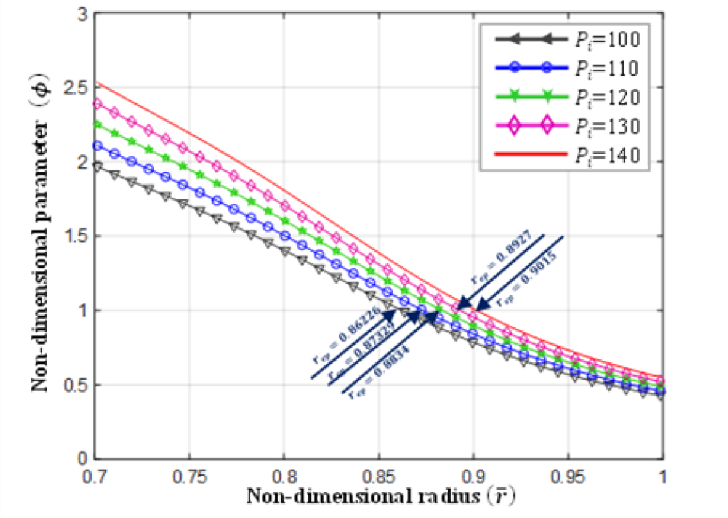

Fig. 16
Changes of dimensionless parameter ϕ for different internal pressure.

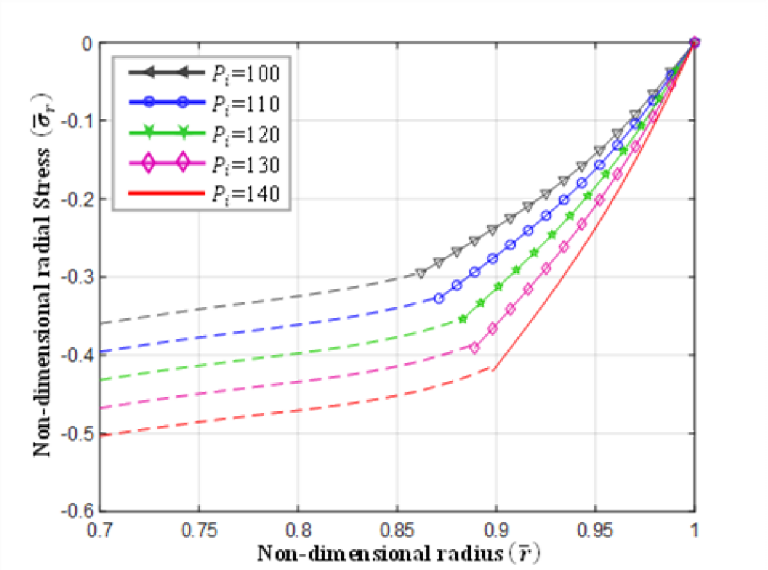

Fig. 17
Radial stress in Magneto-Thermo-Elastic-Plastic FM cylinder for different internal pressure.

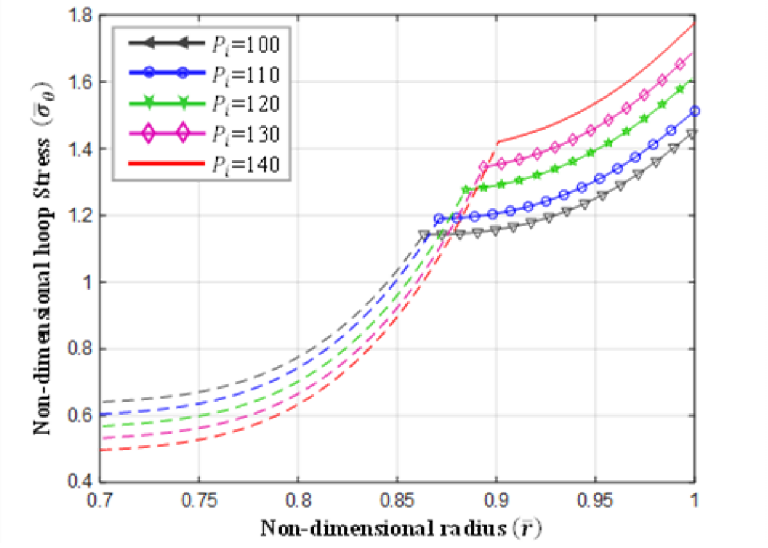

Fig. 18
Hoop stress in Magneto-Thermo-Elastic-Plastic FM cylinder for different internal pressure.

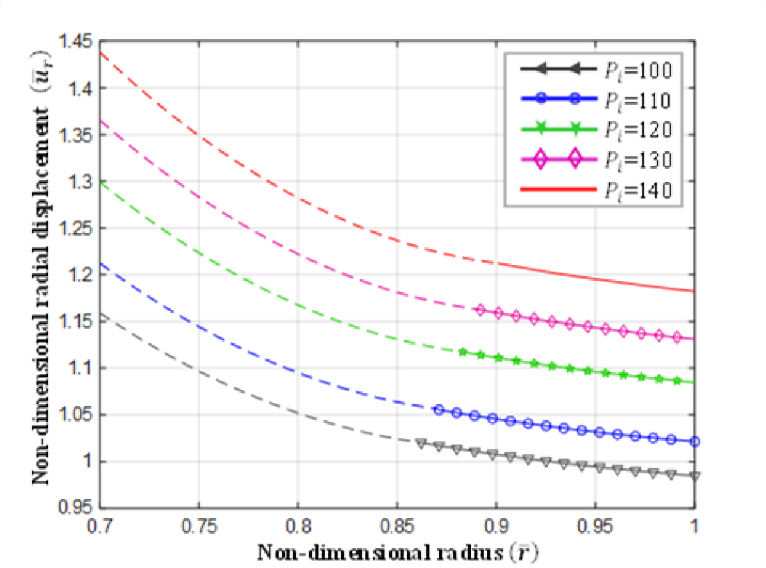

Fig. 19
Radial displacement in Magneto-Thermo-Elastic-Plastic FM cylinder for different internal pressure.

The effect of different radius ratio on deformation, as shown in Figures 20–24. Figure 20 shows that by increasing radius ratio, the plastic radius also increased. One known from the curves of Figures 21–23 that by increasing radius ratio, the plastic region increases.

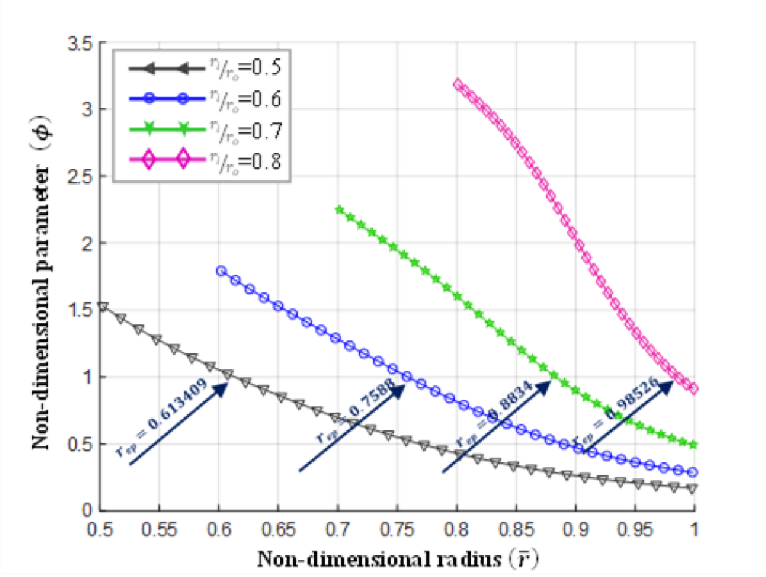

Fig. 20
Changes of dimensionless parameter φ for different radius ratio.

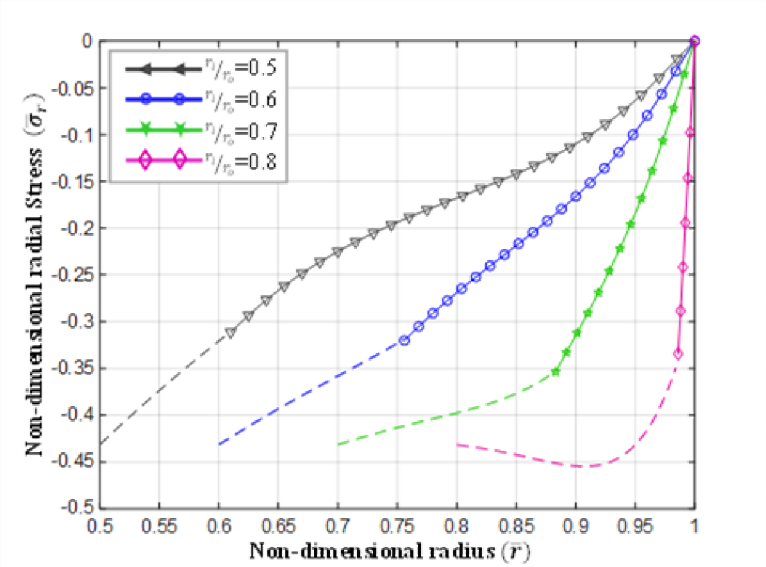

Fig. 21
Radial stress in Magneto-Thermo-Elastic-Plastic FM cylinder for different radius ratio.

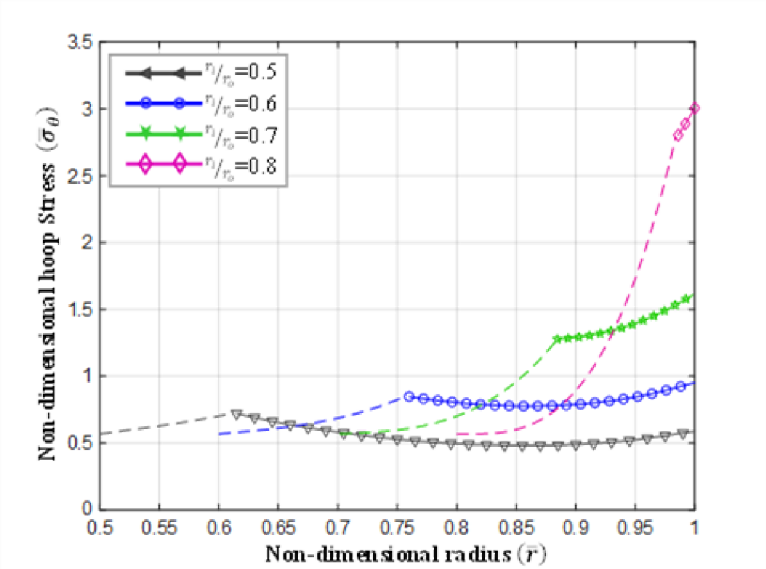

Fig. 22
Hoop stress in Magneto-Thermo-Elastic-Plastic FM cylinder for different radius ratio.

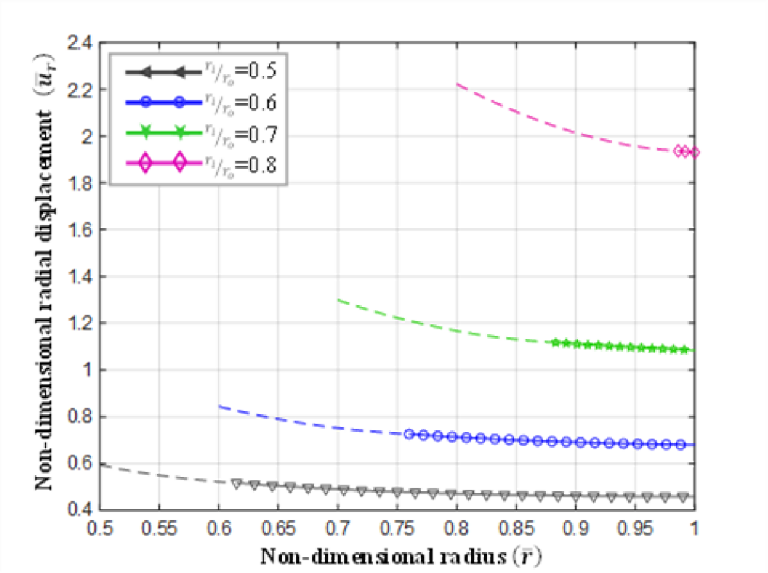

Fig. 23
Radial displacement in Magneto-Thermo-Elastic-Plastic FM cylinder for different radius ratio.

As a final result, Figures 24−27 display the dimensionless parameter ϕ, radial, hoop stresses and radial displacement for four values of magnetic intensity. It is observed from Figures 24-26 that the different magnetic intensity insignificant influences the dimensionless parameter and stresses.

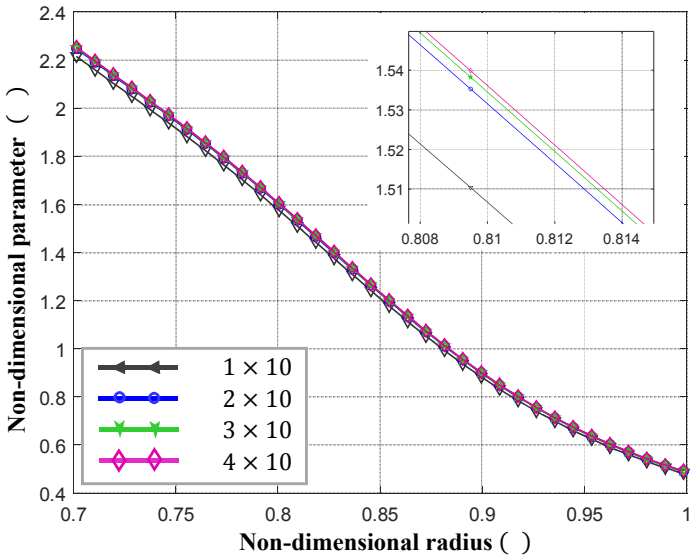

Fig. 24
Changes of dimensionless parameter ϕ for different magnetic intensity.

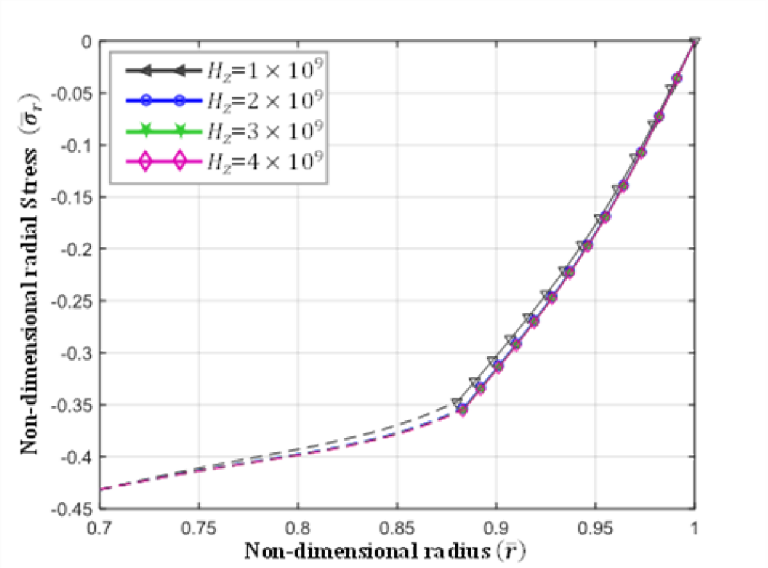

Fig. 25
Radial stress in in Magneto-Thermo-Elastic-Plastic FM cylinder for different magnetic intensity.

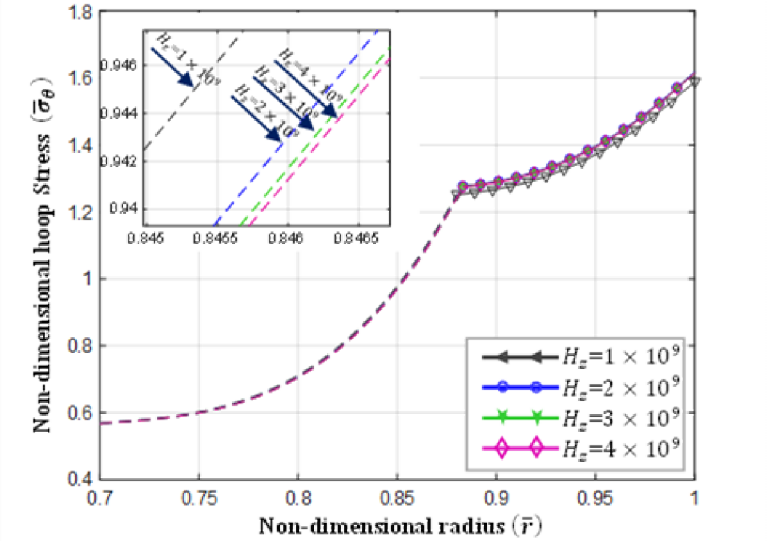

Fig. 26
Hoop stress in in Magneto-Thermo-Elastic-Plastic FM cylinder for different magnetic intensity.

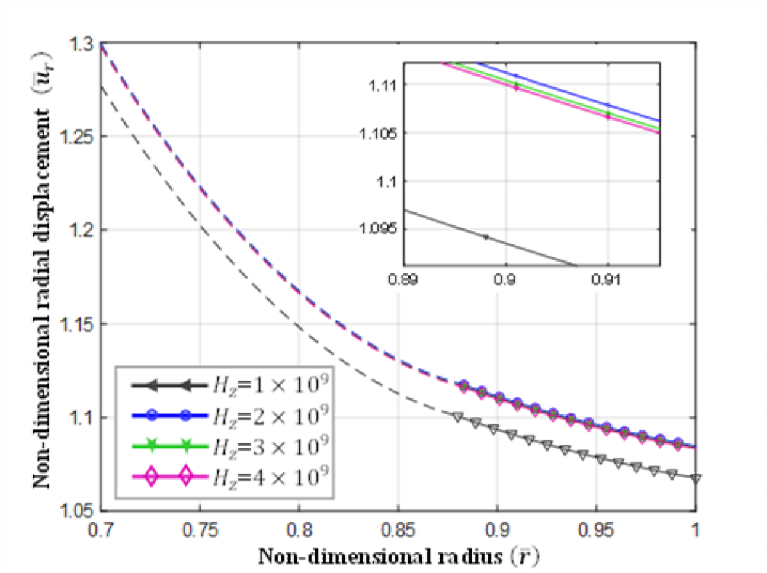

Fig. 27
Radial displacement in in Magneto-Thermo-Elastic-Plastic FM cylinder for different magnetic intensity.

8. CONCLUSIONS

The Thermo-Magneto-Elastic and Thermo-Magneto-Elastic-Plastic plane strain solutions for Al/ZrO_2 has been presented. In this way, the elastic and partially plastic response of FM cylinder has been investigated. The main purpose of this study is Elastic-Plastic analysis. For the sake, Tresca's yield criterion are used. Results show that yielding becomes at the inner surface as a result of loading conditions and selected materials for metal and ceramic phases.

1) The curves disclosed that the value of $\bar{\sigma}_r$ and $\bar{\sigma}_\theta$ decrease as increasing of β. the value of grading index has little effect on the amount of radial displacement in the Thermo-Magneto-Elastic analysis.
2) The elastic-plastic boundary radius increases as the increasing of β, temperature, pressure, radius ratio and magnetic intensity vector.
3) It is seen that the value of $\bar{\sigma}_r$ and $\bar{\sigma}_\theta$ decrease as the increasing of β.
4) It can be found from the curves that the value of $\bar{\sigma}_r$ decrease with the increase temperature, pressure and radius ratio whereas the amount of $\bar{\sigma}_\theta$, first decrease then increase toward the outer surfaces.
5) We indicated that magnetic intensity vector has little effect on the stresses and displacement distributions.

Nomenclature

E	The modulus elasticity
H_z	Magnetic intensity
K	Heat conductivity
P_r	Mechanical property
P_i	Material property at the inner radius
P_o	Material property at the outer radius
r	The radius of the magnetoelastic cylinder
r_i	Inner radius
r_o	Outer radius
u_r	Radial displacement
X_i	Constant parameter/ integration constant
α	Thermal coefficient
β	Grading index
ε	Strain
υ	Poisson's ratio
μ	Magnetic permeability
σ	Stress
σ_y	Yield stress

REFERENCES

[1] R. M. Mahamood, E. T. A. Member, M. Shukla, and S. Pityana, "Functionally Graded Material : An Overview," vol. III, no. January, 2012.

[2] X. Li, P. Li, and G. Kang, "Axisymmetric thermo-elasticity field in a functionally graded circular plate," 2012, doi: 10.1177/1081286512442437.

[3] Y. Fukui, Y. Yammanaka, "Elastic Analysis for Thic-Walled Tubes of Functionally Graded Material Subjected to Internal Pressure," *JSME Int. J.*, vol. 35, no. 5, pp. 683–686, 1991.

[4] M. Jabbari, M. Sohrabpour, S. Eslami, "Mechanical and thermal stresses in a functionally graded hollow cylinder due to radially symmetric loads," *J. Press. Vessel. Pip.*, vol. 79, no. 7, pp. 493–497, 2002.

[5] N. Tutuncu and M. Ozturk, "Exact solutions for stresses in functionally graded pressure vessels," vol. 32, pp. 683–686,

2001.
[6] M. R. Eslami, M. H. Babaei, and R. Poultangari, "Thermal and mechanical stresses in a functionally graded thick sphere," vol. 82, pp. 522–527, 2005, doi: 10.1016/j.ijpvp.2005.01.002.
[7] K. Abrinia, H. Naee, "New Analysis for The FGM Thick Cylinders Under Combined Pressure and Tempreture Loading," *Am. J. Appl. Sci.*, pp. 852–859, 2008.
[8] X. Li, X, Peng, "A Pressurized Functionally Graded Hollow Cylinder with Arbitrarily Varying Material Properties," *J. Elast.*, 2009, doi: DOI 10.1007/s10659-009-9199-z A.
[9] X. L. Peng and X. F. Li, "Thermoelastic analysis of a cylindrical vessel of functionally graded materials," *Int. J. Press. Vessel. Pip.*, vol. 87, no. 5, pp. 203–210, 2010, doi: 10.1016/j.ijpvp.2010.03.024.
[10] Z. Li, Y. Xu, and D. Huang, "Accurate solution for functionally graded beams with arbitrarily varying thicknesses resting on a two-parameter elastic foundation," *J Strain Anal.*, 2020, doi: 10.1177/0309324720922739.
[11] G. J. Nie, Z. Zhong, and R. C. Batra, "Material tailoring for functionally graded hollow cylinders and spheres," *Compos. Sci. Technol.*, vol. 71, no. 5, pp. 666–673, 2011, doi: 10.1016/j.compscitech.2011.01.009.
[12] R. Seifi, "EXACT AND APPROXIMATE SOLUTIONS OF THERMOELASTIC STRESSES IN FUNCTIONALLY GRADED CYLINDERS," *J. Therm. Stress.*, vol. 38, pp. 1163–1182, 2015, doi: 10.1080/01495739.2015.1073513.
[13] W. Q. Chen, "Stress distribution in a rotating elastic functionally graded material hollow sphere with spherical isotropy," *J Strain Anal.*, no. June 1999, pp. 13–20, 2015.
[14] M. Allam, R, Trntawy, A, Zenkour, "THERMOELASTIC STRESSES IN FUNCTIONALLY GRADED ROTATING ANNULAR DISKS WITH VARIABLE THICKNESS," *J. Theor. Appl. Mech. 56,* vol. 56, pp. 1029–1041, 2018, doi: 10.15632/jtam-pl.56.4.1029.
[15] J. W. W. S. . Xie, S. Hao, "Analytical solution of stress in functionally graded cylindrical/spherical pressure vessel," *Appl. Mech.*, 2021.
[16] H. Mohamed, A. Abdalla, D. Casagrande, and L. Moro, "Thermo-mechanical analysis and optimization of functionally graded rotating disks," *J Strain Anal.*, 2020, doi: 10.1177/0309324720904793.
[17] H. Dai, Y M. Fu, Z M. Dong, "Exact solutions for functionally graded pressure vessels in a uniform magnetic fiel," *Int. J. Solids Struct.*, pp. 5570–5580, 2005, doi: 10.1016/j.ijsolstr.2005.08.019.
[18] H. L. Ã. Dai and Y. M. Fu, "Magnetothermoelastic interactions in hollow structures of functionally graded material subjected to mechanical loads," vol. 84, pp. 132–138, 2007, doi: 10.1016/j.ijpvp.2006.10.001.
[19] A. Ghorbanpour, S. Amir, "Magneto-Thermo-Elastic Stresses and Perturbation of Magnetic Field Vector in a Thin Functionally Graded Rotating Disk," *J. Solid Mech.*, vol. 3, no. 4, pp. 392–407, 2011.
[20] P. Sarkar, A, Rahman, "Effect ofmagnetic field on the thermo-elastic response of a rotating FGM Circular disk with non-uniform thickness," *J. Strain Anal.*, pp. 1–16, 2021, doi: 10.1177/03093247211005215.
[21] M. Z. Nejad, M. Jabbari, and M. Ghannad, "A general disk form formulation for thermo-elastic analysis of functionally graded thick shells of revolution with arbitrary curvature and variable thickness," *Acta Mech.*, vol. 228, no. 1, pp. 215–231, 2017, doi: 10.1007/s00707-016-1709-z.
[22] A. N. Eraslan and T. Akis, "Plane strain analytical solutions for a functionally graded elastic – plastic pressurized tube," vol. 83, pp. 635–644, 2006, doi: 10.1016/j.ijpvp.2006.07.003.
[23] T. Akis, "Elastoplastic analysis of functionally graded spherical pressure vessels," *Comput. Mater. Sci. J.*, vol. 46, pp. 545–554, 2009, doi: 10.1016/j.commatsci.2009.04.017.
[24] A. Ozturks, M, Gulgec, "Elastic–plastic stress analysis in a long functionally graded solid cylinder with fixed ends subjected to uniform heat generation," *Int. J. Eng. Sci.*, vol. 49, pp. 1047–1061, 2011, doi: 10.1016/j.ijengsci.2011.06.001.
[25] S. Rash Ahamdi, "Thermo-elastic/plastic semi-analytical solution of incompressible functionally graded spherical pressure vessel under thermo-mechanical loading," *Springer*, pp. 161–173, 2011, doi: 10.1007/s00707-011-0512-0 S.
[26] Z. Mazarei and M. Z. Nejad, "Thermo-Elasto-Plastic Analysis of Thick-Walled Spherical," *Int. J. Appl. Mech.*, vol. 8, no. 4, pp. 1–25, 2016, doi: 10.1142/S175882511650054X.
[27] S. Alikarami, A, Parvizi, "Elasto-plastic analysis and finite element simulation of thick-walled functionally graded cylinder subjected to combined pressure and thermal loading," *Sci. Eng. Compos. Mater.*, 2016, doi: 10.1515/secm-2015-001.
[28] P. Shi and J. Xie, "Exact solution of magneto-elastoplastic problem of functionally graded cylinder subjected to internal pressure," *Appl. Math. Model.*, vol. 123, pp. 835–855, 2023, doi: 10.1016/j.apm.2023.08.014.
[29] H. L. Dai and X. Wang, "Dynamic responses of piezoelectric hollow cylinders in an axial magnetic field," vol. 41, pp. 5231–5246, 2004, doi: 10.1016/j.ijsolstr.2004.04.019.
[30] E. Mahdavi, A. Ghasemi, and R. Akbari, "Elastic – plastic analysis of functionally graded rotating disks with variable thickness and temperature-dependent material properties under mechanical loading and unloading," *Aerosp. Sci. Technol.*, vol. 59, pp. 57–68, 2016, doi: 10.1016/j.ast.2016.10.011.
[31] A. Dini, M. A. Nematollahi, and M. Hosseini, "Analytical solution for magneto-thermo-elastic responses of an annular functionally graded sandwich disk by considering internal heat generation and convective boundary condition," *Journal of Sandwich Structures and Materials*, vol. 23, no. 2. pp. 542–567, 2021. doi: 10.1177/1099636219839161.